Operation of a Hybrid Modular Multilevel Converter during Grid Voltage Unbalance

Emmanuel K. Amankwah*, Alan J. Watson, and Jon C. Clare

Power Electrnics, Machines and Control Research Group, Faculty of Engineering,

The University of Nottingham, Nottingham, UK, NG7 2RD

* Emmanuel.amankwah@nottingham.ac.uk

Abstract: The recently proposed parallel hybrid modular multilevel converter is considered to be a low loss, low component count converter with soft switching capability of the 'main' H-bridge. The converter has similar advantages to other emerging modular multilevel converter circuits being considered for HVDC power transmission and can be made compact which is desirable for offshore application. However, during ac network unbalance the individual 'chain-links' exchange unequal amounts of power with the grid which requires appropriate remedial action. This paper presents research into the performance of the converter and proposes a suitable control method that enables the converter to operate during grid voltage unbalance. The proposed control concept involves the use of asymmetric third harmonic voltage generation in the 'chain-links' of the converter to redistribute the power exchanged between the individual 'chain-links' and the grid. Mathematical analysis and simulation modelling with results are presented to support the work described.

1. Introduction

Modular multilevel voltage source converters (M2LC) are being developed for HVDC and FACTS applications [1-8]. These converters are expected to offer significant benefits over classical HVDC technology utilising Line Commutated Converters (LCCs): - improve the quality of the AC current and voltage waveforms while subjecting the semiconductor devices to low stress [9]. These converters are scalable and can be adapted to many high power and high voltage applications. The advantages of M2LCs make them very attractive for HVDC and FACTs applications; a number of which are currently in operation and many more are planned [10, 11]. In the last decade a number of hybrid modular multilevel voltage source converters [4, 6-8, 12] have been introduced and extensively investigated - all in the attempt to obtain an optimum modular converter topology and make available the advantages of VSCs for HVDC and FACTS applications.

Although, multilevel converters such as the neutral point clamped (NPC) [13] and the flying capacitor converter (FCC) [14] have been investigated for HVDC applications [15] [16], their implementation has been limited by technical challenges. The topological requirement of increasing the number of blocking devices with increasing

number of voltage levels in the NPC among other practical challenges (such as uneven loss distribution in the devices) makes practical implementation of the circuit above three level less promising. As investigated in [16, 17], the volume of capacitance required increases with increasing voltage levels with the FCC. Also, there are other challenges of balancing the voltage on the flying capacitors during converter operation.

The modular multilevel converter (M2LC) [9, 18] offers some interesting advantages for high voltage/power applications:- such as high efficiency, modularity, scalability and high quality voltage and current waveforms. However, the M2LC requires complicated control scheme to ensure that the voltages on the floating capacitors are maintained within a tight tolerant band for sustainable converter operation [19] and the number of submodules and the capacitance required for a particular application is significantly higher [20]. When half bridge (HB) submodules are used, the semiconductor efficiency of the M2LC is significantly improved but the system is not able to respond to DC side faults [21] which is a much desired feature in emerging multi-terminal HVDC systems. Using full bridge (FB) submodules allows VSC HVDC system based on M2LC to quickly respond to DC side faults. However, this practice increases the initial investment cost as well as the system running cost as the conduction loss is significantly increased [21, 22].

The Alternate arm converter (AAC) [6], a hybrid of the M2LC which employs FB submodules and director switches is capable of blocking DC side faults [23] and improve the capacitor and submodule requirements as compared to the M2LC with FB submodules [20]. However, the converter efficiency and volume can still be improved. An alternate arrangement of the AAC is investigated in [8, 24, 25]. In the alternate arrangement, the voltage shaping submodules are on the AC side and the converter is connected to the DC network through a standard two-level converter arrangement. This provides an opportunity to optimise the number of submodules required. However, the devices in the two-level converter are hard switched, resulting in high switching losses and also the problem of dynamic voltage sharing among the devices in the two-level converter [12].

As part of the efforts towards achieving an efficient modular converter topology for the emerging HVDC and FACTS market, the parallel hybrid modular multilevel voltage source converter (PH-M2L-VSC) [7] was proposed. Research into the performance of the converter in a balanced network is presented in [7, 26-30]. The authors of [31] investigated the operation of the converter with a depressed AC voltage by introducing voltage notches in the AC

voltages which has an effect on the DC bus voltage similar to the staggered voltage operation of the converter chain-links in [5]. Although, voltage support operation of the converter has been validated using the concept, a method of energy management is yet to be validated. The converter uses a cascade of half bridge submodules to synthesise a full wave rectified multilevel waveform impressed on it by the operation of the associated main H-bridge during balanced network operations. At the zero crossing of the "chain-link" voltage, the 'main' H-bridge units are soft switched to "unfold" the chain-link voltage into AC at the network frequency. This provides the converter with a desired characteristic of soft switching the devices in the arms of the "main" H-bridge.

The topological arrangement of the converter also favours the use of less energy storage components, making it more compact and more desirable for offshore applications. Other advantages of the converter include high efficiency [28, 31] and fewer devices as compared to a standard MMC. Therefore the running cost of the converter is expected to be significantly lower.

In this paper, operation of the PH-M2L-VSC when connected to an unbalanced grid is investigated. Mathematical analysis and simulation models are used to describe the converter operating characteristics during unbalanced operation. It is shown that the converter chain-links exchange unequal amounts of power with the grid under unbalanced conditions.

A control algorithm that redistributes the power exchanged between the individual chain-links and the grid is proposed. The proposed concept involves the use of asymmetric third harmonic voltage control in the chain-link voltages to avoid mal-operation of the converter during unbalance. From the GB Grid Code and ER P16, the limit of such unbalance that should be tolerated in the system should not exceed 2%. Any amounts of negative sequence exceeding such limits would be classified as fault. However, the work presented in this paper is validated up to 5% unbalance to enable the transition between different control schemes that may be required for converter operation during different scenarios of converter operation.

2. Converter Topology and Basic Operation

As shown in Figure 1, the PH-M2L-VSC is composed of a chain-link arrangement and an associated "main" H-bridge unit for each phase. A chain-link unit is composed of series connection of a number of half bridge submodules. The three converter chain-links connected in series on the DC side operate to support the DC bus and are thus required to provide a proportionate DC component which supports the DC voltage always. On the AC side, the three converter phases are decoupled using a transformer configuration with open windings. On the DC side, the converter is connected to the DC network through a reactor. The reactor on the DC side helps reduce the amount of characteristic harmonics in the DC network.

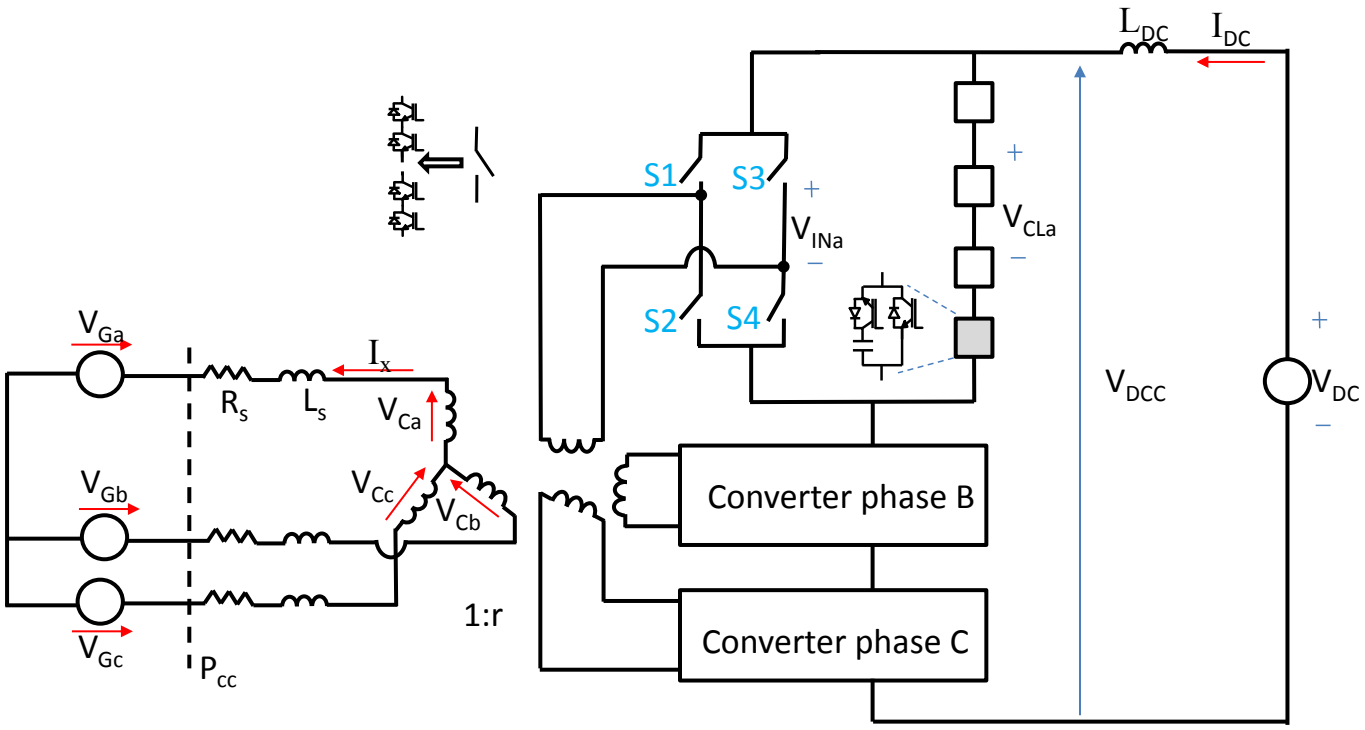

Figure 1: Converter Topology

The operation of the PH-M2L-VSC can be illustrated with Figure 1 and considering that the converter is connected to an AC system which impresses the voltage in (1) on the AC terminal of the converter.

Given that in this application, the 'main' H-bridges are to be soft switched at the zero voltage crossing of the converter

$$V_x = V\sin\left(\omega t - k\frac{2\pi}{3}\right), \quad k \in \{0,1,2\} \qquad (1)$$

AC voltage, the rectified voltage at the DC input of the 'main' H-bridges can be described by (2).

The soft switching capability of the 'main' H-bridge is implemented by simply switching the two diagonal arms of

$$V_{CLx} = V_{RECx} = V\left|\sin\left(\omega t - k\frac{2\pi}{3}\right)\right|, \quad k \in \{0,1,2\} \text{ and } x \in \{a,b,c\} \tag{2}$$

the 'main' H-bridge into or out of conduction. For instance given Figure 1, the switches S1 and S4 will be turned ON (S2 and S3 OFF) when (1) is positive and S2 and S3 ON when (1) is negative. With this implementation, the arms of the 'main' H-bridge are switched only at the fundamental frequency of the AC system. With the 'main' H-bridge operated as a soft switched 2-level converter which 'unfolds' the voltage imposed at its DC input, tracking of the sinusoidal AC voltage is achieved with the use of the series connected Chain-Links (CL). The Chain-Links operate to track the full wave rectified sinusoids at the DC input of the 'main' H-bridge to facilitate synthesises of the required high quality AC voltage waveforms. This implies V_{CLx} is equal to V_{INx}. The DC component of the voltage synthesised by the three series connected CLs can be obtained as (3) and the DC contribution by the three CLs expressed by (4). Neglecting the effect of the DC reactor, for a given DC network the operation of the three chain-links needs to generate

$$\bar{V}_{CLx} = \frac{2}{\pi}V \tag{3}$$

$$\bar{V}_{DCC} = \sum_{x=a,b,c}\bar{V}_{CLx} = \frac{6}{\pi}V \tag{4}$$

enough voltage to support the DC bus voltage. Considering this constraint, the amplitude of the voltage that can be synthesised by the converter is directly related to the DC bus voltage. This therefore limits the operating range of the converter to a fixed modulation index (MI). Methods of decoupling the AC voltage amplitude whilst supporting the DC voltage have been investigated using the addition or subtraction of triplen harmonic voltages. With the concept of triplen harmonic voltage injection, considering only the dominant component in this example, the decoupled CL voltage in each of the phases V_{CLDx} can be described with (5).

$$V_{CLDx} = V\left|\sin\left(\omega t - k\frac{2\pi}{3}\right) + \alpha\sin(3\omega t)\right|, \quad k \in \{0,1,2\} \text{ and } x \in \{a,b,c\} \tag{5}$$

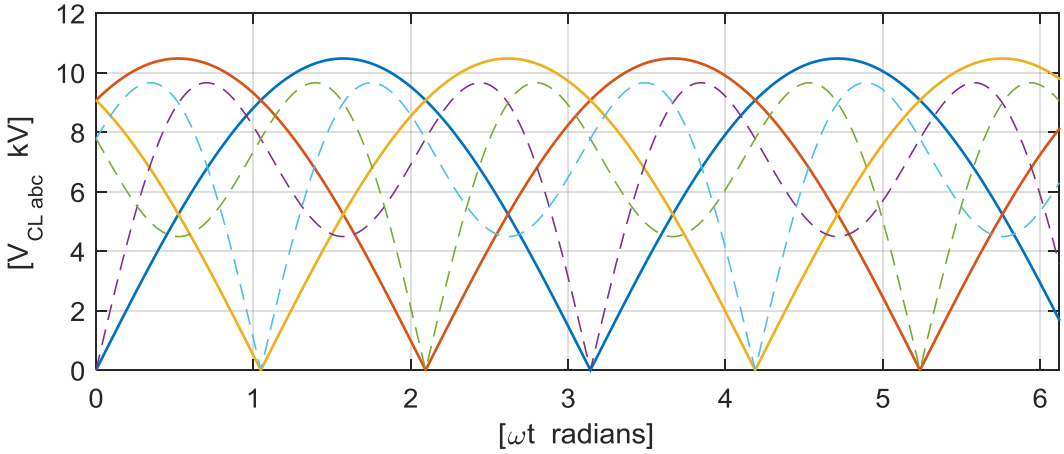

Figure 2: Converter Chain-Link Voltages with α= 0 (continuous lines) and with α=0.5 (dashed lines)

With this implementation, the DC voltage in each CL and the total across the three CLs can be derived as (6).

$$\bar{V}_{CLDx} = \frac{2}{\pi} V\left(1+\frac{\alpha}{3}\right)$$
$$\bar{V}_{DCC} = 3\bar{V}_{CLDx} = \frac{6}{\pi} V\left(1+\frac{\alpha}{3}\right) \quad (6)$$

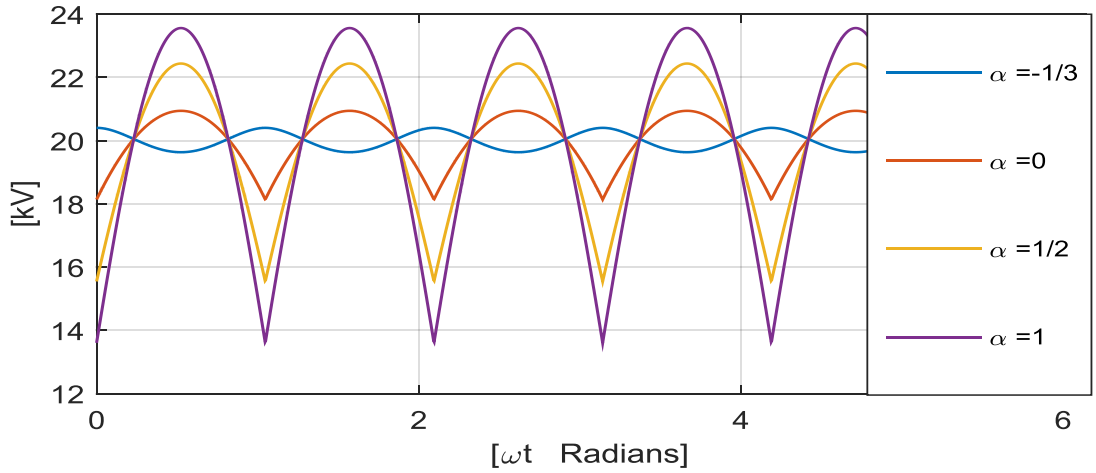

Figure 3: Total Chain-Link Voltage with varying α

Therefore, with the use of the third harmonic voltage, the DC bus voltage $\bar{V}_{DCC}$ can be maintained with varying AC voltage amplitude at the converter terminal. Given that the CLs cannot generate negative voltages the amount of third harmonic voltage that the CLs can accepts has been shown to be within the range of $-1/3 \le \alpha \le 1$, limiting the MI range (7) to $0.785 \le MI \le 1.178$.

All these analysis are presented in line with a balanced three phase system. In such operation, the voltages synthesised

$$MI = \frac{2\pi}{6(1+\alpha/3)} \tag{7}$$

by the three converter CLs are displaced 120 electrical degrees apart. The 120 electrical degree phase shift in the "chain-link" voltages results in attendant 6n harmonic voltage in the summed total "chain-link" voltage as shown in Figure 3. Though the techniques of [30, 32] were developed for symmetrical network operations, they can still be used under unbalanced conditions for ripple reduction, but because of asymmetry, the cancellation will not be as effective as it will be in a symmetrical system. Further quantitative analysis of the ripple reduction under unbalanced conditions is outside the scope of this paper.

3. Converter Operation during Grid Voltage Unbalance

Investigation of the operation of the PH-M2L-VSC is undertaken considering that the neutral of the converter transformer will not be grounded in implementations where voltage ratio control is achieved with the use of triplen harmonic voltage injection. Therefore there is no circulation of zero sequence components in the converter during unbalance. We consider a system where the grid voltage is composed of positive and negative sequence voltages during unbalance. The unbalance factor (β) represents the ratio of the amplitude of the negative to the positive sequence voltages in the circuit [32] [33]. It is considered that the converter is controlled to inject negative sequence voltage proportionate to that in the grid to avoid the circulation of negative sequence current. By so doing, it can be assumed that the current through the system is composed of positive sequence only.

The voltage at the converter terminal is therefore considered to contain a proportionate amount of negative sequence voltage as in (8).

Which impose the voltages described in (9) on the individual converter chain-links.

$$V_{unbx} = V\left(\sin\left(\omega t - k\frac{2\pi}{3}\right) + \beta\sin\left(\omega t + k\frac{2\pi}{3}\right)\right), \quad k \in \{0,1,2\} \tag{8}$$

$$V_{CL\_unbx} = V\left|\left(\sin\left(\omega t - k\frac{2\pi}{3}\right) + \beta\sin\left(\omega t + k\frac{2\pi}{3}\right)\right)\right|, \quad k \in \{0,1,2\} \tag{9}$$

For ease of illustration, it is assumed here that the unbalance does not result in extra phase shift between the positive and negative sequence reference frames and therefore the zero crossing instants on phase 'a' are not affected. However, the zero crossing time instants of phases 'b' and 'c' are shifted according to the degree of unbalance in the system.

The zero crossing time instants for the voltage on chain-link '*b*' can be obtained as t_b (10) and $t`_b$ (11). Similar equations can be derived for the zero crossing time instants of the voltages on chain-link 'c'.

Considering that the converter is exchanging only active power with the grid, the current through the system can be

$$t_b = \frac{1}{\omega}\left(\frac{2\pi}{3} + \arcsin\left(\frac{\sqrt{3}}{2}\right)\frac{\beta}{\left(1+\beta^2+\beta\right)^{\frac{1}{2}}}\right), \tag{10}$$

$$t_b = \frac{1}{\omega}\left(-\frac{\pi}{3} + \arcsin\left(\frac{\sqrt{3}}{2}\right)\frac{\beta}{\left(1+\beta^2+\beta\right)^{\frac{1}{2}}}\right), \tag{11}$$

represented by (12).

With an unbalance component of β on the converter voltage, the peak voltage imposed on the chain-links can be

$$I_x = I\sin\left(\omega t - k\frac{2\pi}{3}\right), \quad k \in \{0,1,2\} \tag{12}$$

obtained as (13) and (14)

The unbalance on the AC side affects the DC component of the individual chain-links even when the negative

$$\hat{V}_{cl}{}^{a} = V(1+\beta) \tag{13}$$

$$\hat{V}_{cl}{}^{b} = \hat{V}_{cl}{}^{c} = V\sqrt{\left(1+\beta+\beta^2\right)} \tag{14}$$

sequence voltage introduced by the unbalance is synthesised by the chain-links to prevent the flow of negative sequence currents. The DC component of the imposed chain-link voltages can be derived (15), (16), and (17) for chain-links 'a', 'b' and 'c'.

$$\bar{V}_{cl}{}^{a} = \frac{2V}{\pi}(1+\beta) \tag{15}$$

$$\bar{V}^{b}{}_{cl} = \frac{1}{\pi}V\left(-cos(\omega t_b) + \sqrt{3}\sin(\omega t_b) - \beta\left(\cos(\omega t_b) + \sqrt{3}sin(\omega t_b)\right)\right) \tag{16}$$

$$\bar{V}^{c}{}_{cl} = \frac{1}{\pi}V\left(-cos(\omega t_c) + \sqrt{3}\,sin(\omega t_c) - \beta\left(cos(\omega t_c) + \sqrt{3}sin(\omega t_c)\right)\right) \tag{17}$$

The variation of the DC component of each "chain-link" voltage with increasing unbalance factor is shown in **Figure 4** .

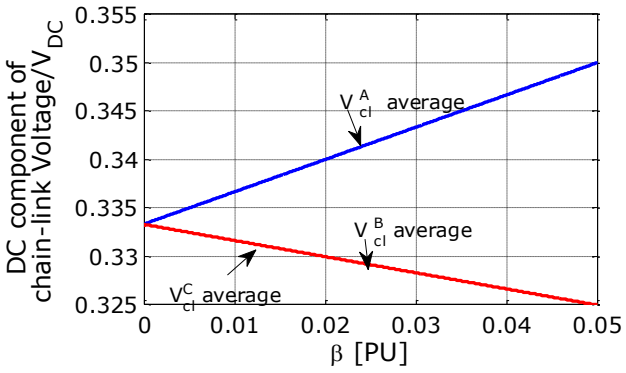

Figure 4: Variation of DC component of each "chain-link" with increasing unbalance factor

Considering β, the active power exchanged between each converter chain-link and the grid can be evaluated as

$$\overline{P^a}_{cl} = \frac{2VI_{DC}}{\pi}(1+\beta) - \left(\frac{1+\beta}{2}\right)VI_p cos\varphi \tag{18}$$

$$\begin{aligned}\overline{P^b}_{cl} = {} & \frac{2VI_{DC}}{\pi}\left(\cos(\omega t_b) - \sqrt{3}\sin(\omega t_b)\right) \\ & - \frac{\beta VI_{DC}}{\pi}\left(\cos(\omega t_b) + \sqrt{3}\sin(\omega t_b)\right) - \frac{VI_p}{2}cos\varphi \\ & + \frac{\beta VI_p}{4}\left(cos\varphi + \sqrt{3}\,sin\varphi\right)\end{aligned} \tag{19}$$

$$\begin{aligned}\overline{P^c}_{cl} = {} & \frac{2VI_{DC}}{\pi}\left(\cos(\omega t_c) + \sqrt{3}\sin(\omega t_c)\right) - \frac{\beta VI_{DC}}{\pi}\left(\cos(\omega t_c) - \sqrt{3}\sin(\omega t_b)\right) \\ & - \frac{VI_p}{2}cos\varphi + \frac{\beta VI_p}{4}\left(cos\varphi - \sqrt{3}\,sin\varphi\right)\end{aligned} \tag{20}$$

Where $\overline{P^a}cl$, $\overline{P^b}cl$, and $\overline{P^c}cl$ refer to the average power in phases a, b, and c.

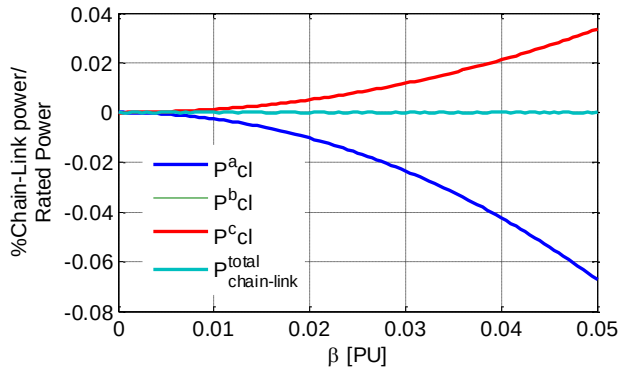

Figure 5: Change in active power in each converter "chain-link" for increasing voltage unbalance factor at unit PF operation for 20MW/20kV (DC), 11kV (AC) system

From the net power exchange in Figure 5, it is clear that a remedial action is required for sustainable operation of the converter during grid voltage unbalance.

4. Proposed Control Concept for Sustained Operation during Grid Voltage Unbalance

It has been shown that the PH-M2L-VSC requires an appropriate remedial action during converter operation with minimal unbalanced grid voltage operation. In [7, 27, 30], the use of triplen harmonics are explored for modulation ratio control in the PH-M2L-VSC allowing PQ control and DC link voltage ripple reduction. In these papers, the studies considered a balanced symmetrical grid with equal amount of triplen harmonic injected in each "chain-link" to allow fundamental frequency ac converter voltage control.

It shall be demonstrated in this paper that by injecting unequal amounts of triplen harmonics in the converter "chain-link" voltages proportional to the degree of unbalance, the operation of the converter can be sustained while maintaining power exchange with the grid. Consider the case where the "chain-links" are to synthesise the unbalance voltages imposed at the AC terminal as in (9) the voltage to be synthesised by the chain-link can be expressed as (21), (22) and (23) for phases a, b, and c.

$$V^{a}{}_{cl} = V|(1+\beta)sin(\omega t) + \alpha_a sin(3\omega t)| \tag{21}$$

$$V^{b}{}_{cl} = V\left|sin\left(\omega t - \frac{2\pi}{3}\right) + \beta sin\left(\omega t + \frac{2\pi}{3}\right) + \alpha_b sin(3\omega t - \psi)\right| \tag{22}$$

$$V^{c}{}_{cl} = V\left|sin\left(\omega t + \frac{2\pi}{3}\right) + \beta sin\left(\omega t - \frac{2\pi}{3}\right) + \alpha_c sin(3\omega t + \psi)\right| \tag{23}$$

Where α_a, α_b, and α_c, are the proportionate third harmonic voltages to be injected for sustainable operation during unbalance. ψ is the compensation term for the phase displacement on phases 'b' and 'c' during the zero voltage soft switching instant due to the unbalance.

From (21), (22) and (23), the new DC component of the "chain-link" voltages can be obtained for each phase as:

$$\overline{V^{a}}_{cl} = \frac{2}{\pi}V\left(1+\beta+\frac{\alpha_a}{3}\right) \tag{24}$$

$$\overline{V^b}_{cl} = \frac{1}{\pi} V \left(-cos(\omega t_b) + \sqrt{3}\, sin(\omega t_b) - \beta \left(cos(\omega t_b) + \sqrt{3}\, sin(\omega t_b) \right) + \frac{2}{3} \alpha_b cos(3\omega t_b - \psi) \right) \tag{25}$$

$$\overline{V^c}_{cl} = \frac{1}{\pi} V \left(-cos(\omega t_c) - \sqrt{3}\, sin(\omega t_c) - \beta \left(cos(\omega t_c) - \sqrt{3}\, sin(\omega t_c) \right) + \frac{2}{3} \alpha_c cos(3\omega t_c + \psi) \right) \tag{26}$$

Under such conditions, the active power exchanged between each converter "chain-link" and the grid without reactive compensation can be expressed for each phase as:

$$\overline{P^a}_{cl} = \frac{2}{\pi} V I_{DC} \left(1 + \beta + \frac{\alpha_a}{3} \right) - \left(\frac{1+\beta}{2} \right) VI \tag{27}$$

$$\overline{P^b}_{cl} = \frac{1}{\pi} V I_{DC} \left(-a - \beta c + \frac{2}{3} \alpha_b cos(3\omega t_b - \psi) \right) - \frac{VI}{4} (2 - \beta) \tag{28}$$

$$\overline{P^c}_{cl} = \frac{1}{\pi} V I_{DC} \left(-b - \beta d + \frac{2}{3} \alpha_c cos(3\omega t_c + \psi) \right) - \frac{VI}{4} (2 - \beta) \tag{29}$$

Where a, b, c and d are described in (30).

$$\begin{aligned} a &= cos(\omega t_b) - \sqrt{3} sin(\omega t_b) \\ b &= cos(\omega t_c) + \sqrt{3} sin(\omega t_c) \\ c &= cos(\omega t_b) + \sqrt{3} sin(\omega t_b) \\ d &= cos(\omega t_c) - \sqrt{3} sin(\omega t_c) \end{aligned} \tag{30}$$

The net power exchanged between the converter chain-link and the grid (27), (28), (29) can be set to be equal and zero as required by using the appropriate values of α_a, α_b, and α_c.

The values for the required third harmonic voltage to be injected for varying amounts of unbalance can be obtained from (31)

$$X = \Lambda^{-1} Y \tag{31}$$

Where

$$X = \begin{bmatrix} \alpha_a \\ \alpha_b \\ \alpha_c \end{bmatrix} \tag{32}$$

And

$$\Lambda = \frac{2}{3}\begin{bmatrix} (2-\beta) & -(1+\beta)cos(3\omega t_b - \psi) & -(1+\beta)cos(\omega t_c + \psi) \\ (2-\beta) & -(4+\beta)cos(3\omega t_b - \psi) & (2-\beta)cos(\omega t_c + \psi) \\ (2-\beta) & (2-\beta)cos(3\omega t_b - \psi) & -(4+\beta)cos(\omega t_c + \psi) \end{bmatrix} \tag{33}$$

$$\gamma = \begin{bmatrix} A \\ B \\ C \end{bmatrix}$$

$$\begin{aligned} A &= -(1+\beta)(4+2\beta) - (1+\beta)^2(\cos(\omega t_b) + \cos(\omega t_c)) + \sqrt{3}(1+\beta)(1-\beta)(\sin(\omega t_b) - \sin(\omega t_c)) \\ B &= 2(1+\beta)(\beta-2) + (1+\beta)(-(4+\beta)\cos(\omega t_b) + (2-\beta)\cos(\omega t_c)) - \sqrt{3}(\beta-1)(-(4+\beta)\sin(\omega t_b) + (2-\beta)\sin(\omega t_c)) \\ C &= 2(1+\beta)(\beta-2) + (1+\beta)((2-\beta)\cos(\omega t_b) - (4+\beta)\cos(\omega t_c)) - \sqrt{3}(1-\beta)((2-\beta)\sin(\omega t_b) + (4+\beta)\sin(\omega t_c)) \end{aligned} \tag{34}$$

In which the components of γ are the unbalance factor dependant constants in the evaluation of (27), (28) and (29) presented in (34).

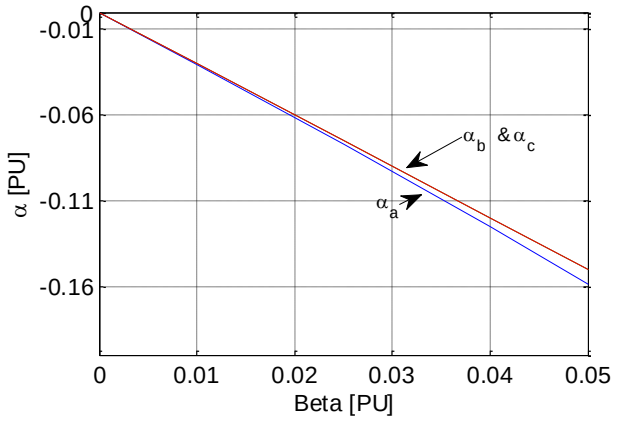

Figure 6: Amount of third harmonic voltage injected in each "chain-link" for increasing unbalance factor

Figure 6 shows the amount of third harmonic components required to sustain converter operation with minimal voltage unbalance (β up to 5%) during normal converter operation. The corresponding power exchanged between the grid

and the converter "chain-link" when the converter operates with the proposed third harmonic injection control is shown Figure 7.

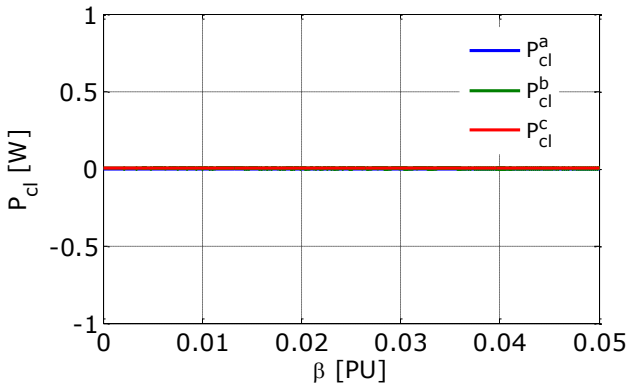

Figure 7: Active power exchanged between the converter "chain-links" and the grid with increasing voltage unbalance factor when the converter operates with the proposed voltage unbalance control

It is evident that the proposed third harmonic injection ensures equal and zero net power exchange between the "chain-links" of the converter and the grid. The asymmetric third harmonic voltage injection therefore ensures 'natural' power balance in each of the converter "chain-links" during unbalanced grid voltage operation. If the amount of asymmetric third harmonic voltage in Figure 6 is considered in the MI range calculation in (7), the new MI range (considering maximum unbalance of 5%) can be obtained from (35) which evaluates to 0.82≤ MI≤1.25.

$$MI = \frac{\pi}{(3+\alpha+\alpha_x)} \tag{35}$$

Modelling and Simulation

The proposed concept has been validated using simulation model of a 20MW 20kV (DC) converter connected to an 11kV grid. Techniques for extracting the reference frame components during unbalance [34] are used to obtain the unbalance factor (β) in the grid and the proportion of asymmetric third harmonic voltage (α_x) required for sustainable operation is evaluated using the control concept discussed in the Section 4.

Table **1** lists the main parameters used in the simulation model.

The model is implemented in PLECS with 10 half bridge submodules in each chain-link and a submodule local storage capacitor of 4mF. Due to the relative low number of submodules used as compared to that which will be

implemented in a practical high power and high voltage application, PWM techniques are implemented to improve the voltage and current fidelity. The modelled converter is validated for operation in a balanced system and an unbalanced system – validating the proposed unbalanced control concept. Figure 8 illustrates the modelled 3 phase converter connected to the grid.

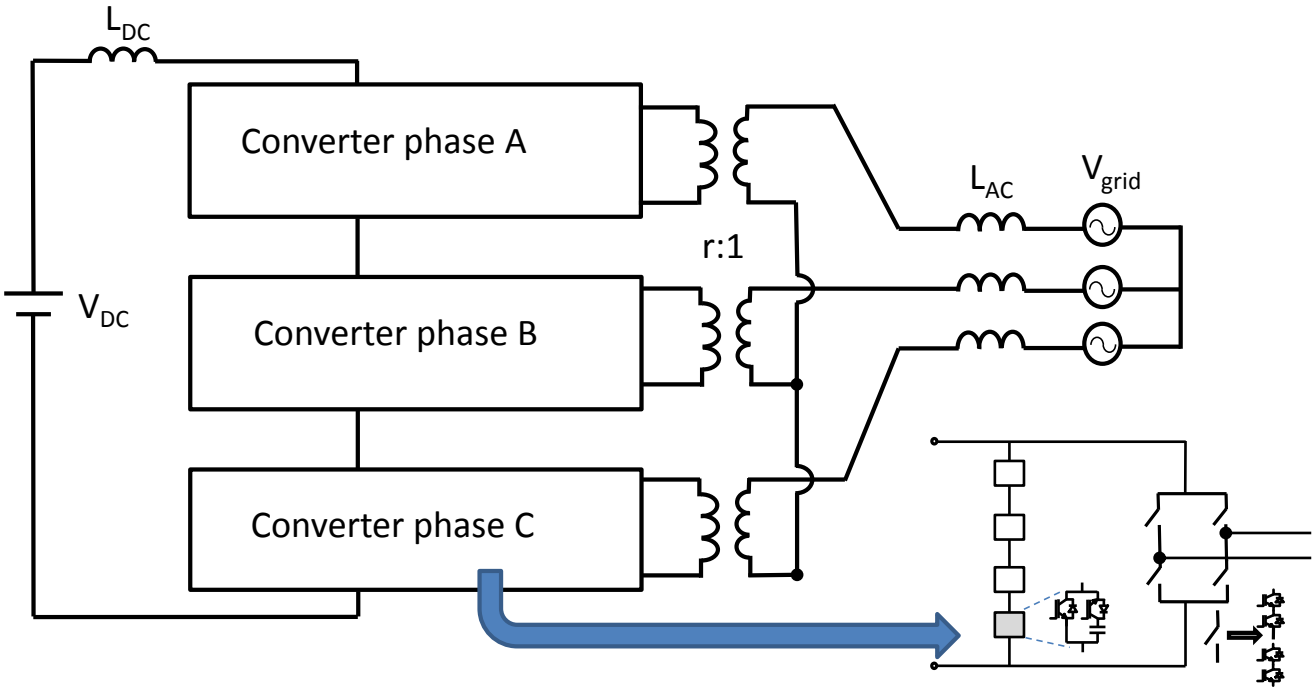

Figure 8: PH-M2L-VSC connected to an unbalanced AC network

Table 1: Simulation parameters

Parameter	Value
Supply voltage (L-L)	11kV
DC bus voltage	20kV
Unbalance factor	1-5 %
Cell capacitance	4mF
DC Link inductance	22.06mH
AC side inductance	2.3mH
Nominal cell capacitor voltage	1.5kV

4.1. Converter Control

In balanced three phase system operation, all the three phase quantities (voltages and currents) are symmetrical. In such applications it is a well-established concept to implement the AC system controllers in a synchronous reference frame (SRF) where the system parameters are transformed to a rotating reference frame using the Park transform [35] which is synchronised to the system frequency. The use of SRF allows the AC quantities to be transformed to DC quantities where classical control schemes such as PI can be applied to achieve the desired performance. However, when there is an unbalance in the AC system, there would be more than one sequence component present in the AC system. In such application, to be able to achieve the benefits of classical control schemes, such as zero steady state error, fast response and fixed switching frequency [36], multiple reference frame control schemes could be applied. In the application of the multiple reference frames schemes, it is essential that the different sequence voltage and current components are well extracted and synchronised to the appropriate reference frame to be able to effect the injection of the corresponding sequence currents.

As this paper considers the control of the converter when there is significant negative sequence voltage in the system (up to 5%) during 'normal' operation, methods of extracting the two sequence components into the respective SRFs are required. The decoupled double synchronous reference frame (DDSRF) concept presented in [34] is adopted to extract the positive and negative sequence voltages and transform to the positive and negative reference frames. Detailed analysis of the decoupled double synchronous reference frame (DDSRF) concept is well presented in [34] and therefore not discussed in here. However, the concept as applied in this publication is illustrated in Figure 9.

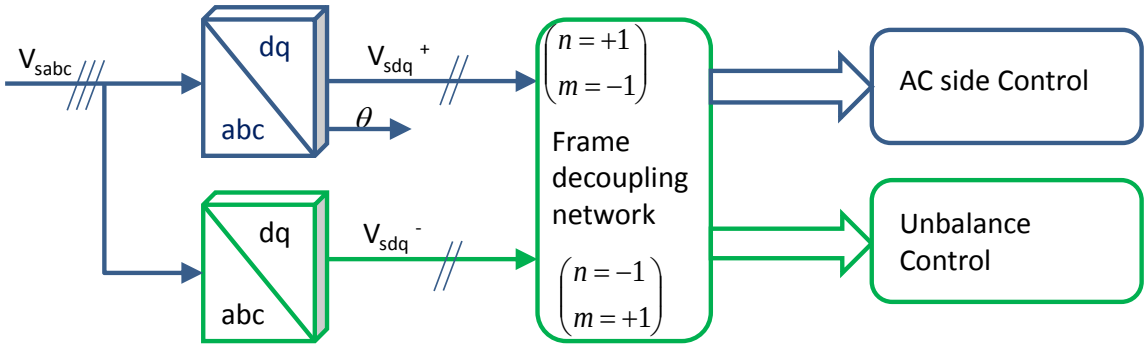

Figure 9: Sequence voltage extraction using the Frame decoupling network

In Figure 9, the unbalance grid voltages are measured and transformed into positive and negative reference frames. The decoupling frame network proposed in [34] in used to extract accurately the ripple free dq components in each frame. The obtained ripple free voltages are used in the AC side control (Figure 10) and the unbalance control technique where the asymmetric third harmonic voltage control is implemented. In the unbalance control block Figure 9, the unbalance factor is obtained from the extracted positive and negative sequence voltages in the grid. Using the obtained unbalance factor, the amount of third harmonic voltage required for the unbalance control is evaluated from (31).

The AC power management scheme Figure 10, controls the power exchanged between the power converter and the AC network by injecting positive sequence currents. The current compensator in Figure 10 is based on PI controllers. The voltage demands from the current controllers are added to the reference grid voltages to obtain the reference converter voltage which is used in the modulation.

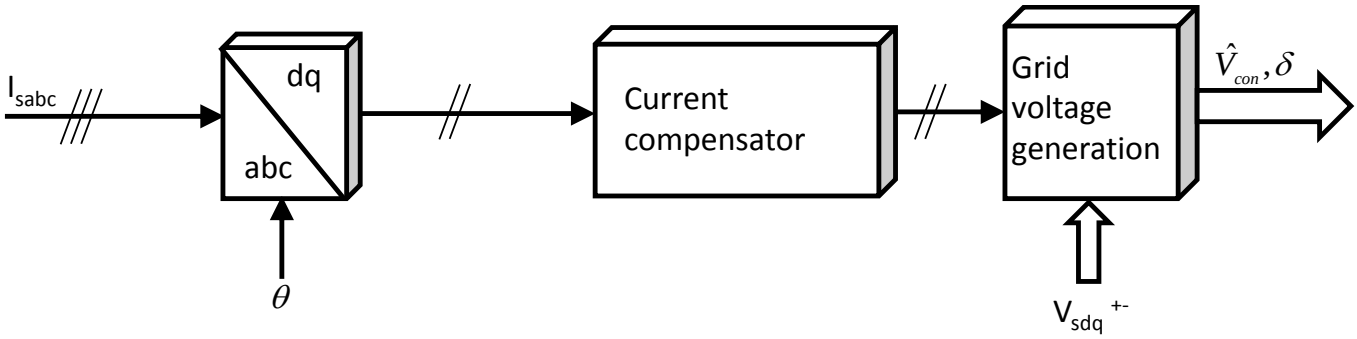

Figure 10: AC power management structure

To ensure that the DC bus voltage of the converter is maintained during balanced and unbalanced operation, the DC side control structure, Figure 11, is implemented. The control structure ensures that the power exchanged between the power converter and the AC network is marched with the power exchanged between the power converter and the DC network. Also, the DC side control ensures that a symmetrical third harmonic voltage is injected to maintain the DC bus voltage at all times during converter operation through a cascade control of the local submodule storage capacitor and the DC current.

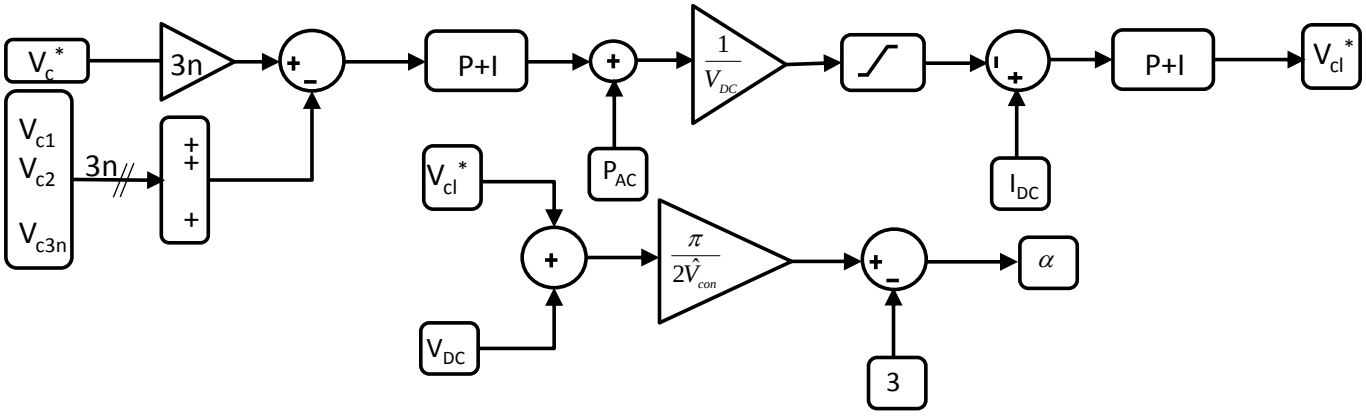

Figure 11: DC side control using symmetrical third harmonic injection

The fundamental AC voltages generated by the AC power management control, the asymmetric third harmonic voltage required for unbalance ratio control and the symmetric third harmonic voltage used for DC voltage ratio control are to be synthesised by the converter Chain-Links. The converter Chain-Link voltages can now be defined as (36)

With the limited number of submodules used in this work, the Chain-Links are controlled with PWM to improve the

$$V_{CL\_x} = \hat{V}_{con}\left|\left(\sin\left(\omega t - k\frac{2\pi}{3}\right) + \alpha\sin(3\omega t) + \alpha_x\sin\left(3\omega t + \psi_x\right) + \beta\sin\left(\omega t + k\frac{2\pi}{3}\right)\right)\right|,\ k \in \{0,1,2\} x \in \{a,b,c\} \quad (36)$$

voltage waveform quality. Multicarrier pulse width modulation schemes such as the phase shifted and the level shifted have been applied to modular multilevel converters [19, 26] and both have shown benefits when applied to low and medium voltage M2LCs. In this paper the level shifted PWM concept presented in [26] is employed to implement the converter cell modulation and to achieve intra-arm local capacitor voltage balancing.

5. Results and Discussion

Results from the simulation model set up to validate the proposed control concepts are presented in Figure 12 to Figure 14. The line currents when the converter exchanges 20MW of power with the grid during 5% unbalance operation are presented in Figure 12(a). It can be observed that the currents are of high quality with non-significant distortion.

Grid voltages during balanced and unbalanced operation are presented in **Figure 12**(b). It can be observed that the presented grid voltages are well balanced until the unbalance is introduced at 100ms from start of the simulation. The

corresponding voltage synthesised by the converter during balanced operation (before 100ms) and unbalanced operation (after 100ms) are shown in **Figure 12**(c).

The submodule capacitor voltages of the "chain-links" are presented in Figure 13. It is shown that before 100ms when the converter exports 20MW with the balanced grid, the voltages on all the capacitors in the three "chain-links" pulsate about same nominal value of 1.5kV.

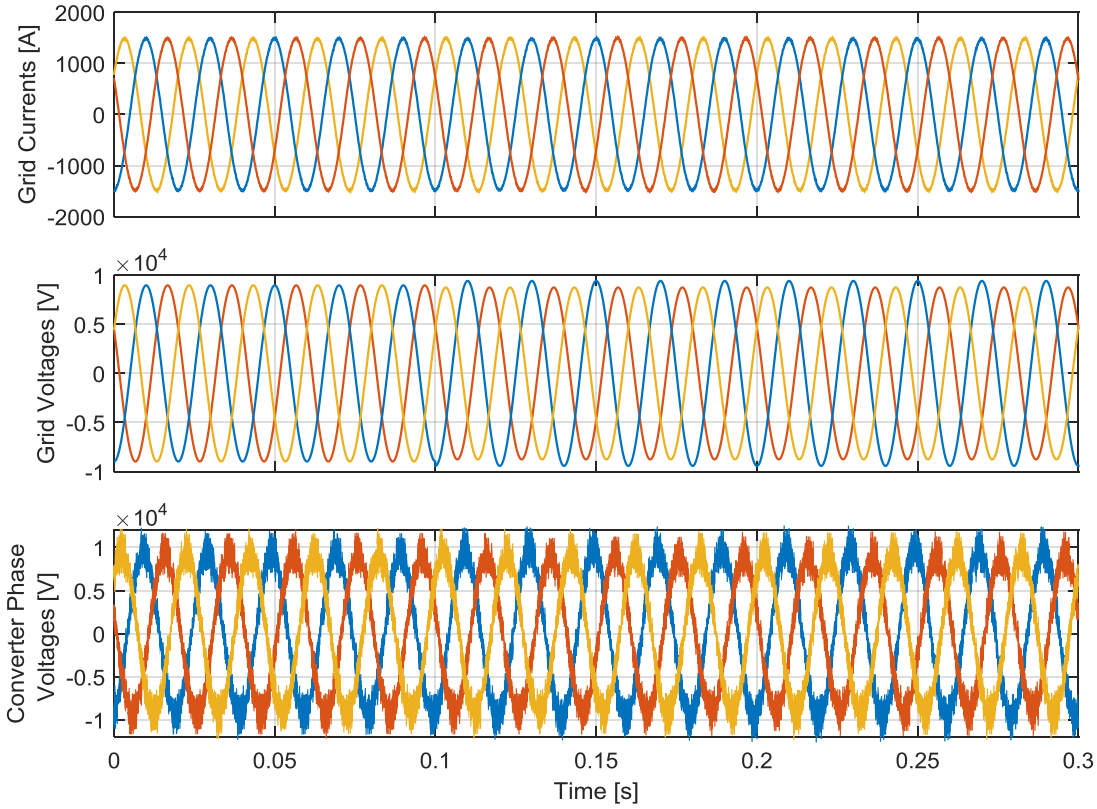

Figure 12: System voltages and current during balanced and unbalanced operation when the converter exchanges 20MW with the grid: (a) Exchanged grid currents, (b) Grid voltages during balanced and unbalanced operation, (c) Converter voltages during balanced and unbalanced operation

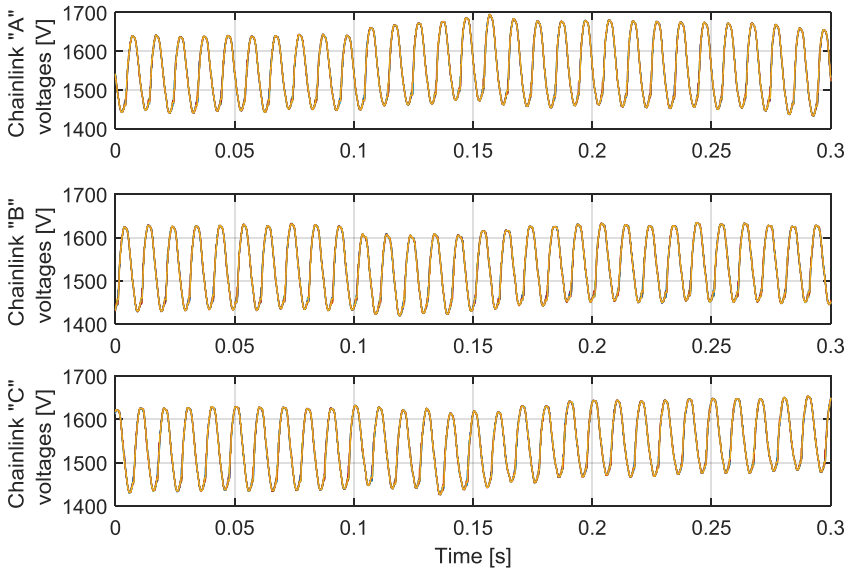

Figure 13: Chain-Link capacitor voltages during balanced and unbalance operations

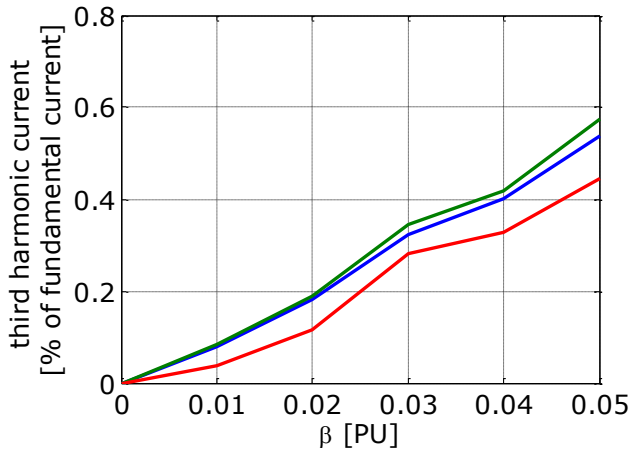

Figure 14: Residual third harmonic current upon application of the unbalance control

However, the effect of the unbalance is observed on the local submodule capacitor voltage from when the unbalance is introduced until the unbalance control is applied at 150ms. Clearly, the effect of the unbalance control with asymmetric third harmonic injection is observed on the submodule capacitor voltage when it is applied 50ms after the unbalance occurs. The effect of the proposed unbalance control concept on the grid currents is shown in Figure 14. It is shown that for unbalances up to 5% the effect of the residual third harmonic current in the grid due to the control concept is less than 0.6%.

6. Conclusion

A novel method for the control of a parallel hybrid modular multilevel converter during voltage unbalance is proposed. It is shown that sustainable operation of the converter can be achieved during unbalance by injecting a proportionate amount of third harmonic (maximum of 16% third harmonic for 5% unbalance factor) into the "chain-links". The proposed method has been validated through mathematical analysis and simulation modelling using PLECS. Results from the simulation model have been presented to support the performance of the converter during grid voltage unbalance.

7. Acknowledgement

The authors gratefully acknowledge the support of Alstom Grid (formerly Areva T&D) in undertaking this research.

8. References

[1] N. Flourentzou, V. G. Agelidis, and G. D. Demetriades, "VSC-Based HVDC Power Transmission Systems: An Overview," *Power Electronics, IEEE Transactions on*, vol. 24, pp. 592-602, 2009.

[2] S. Allebrod, R. Hamerski, and R. Marquardt, "New transformerless, scalable Modular Multilevel Converters for HVDC-transmission," in *Power Electronics Specialists Conference, 2008. PESC 2008. IEEE*, 2008, pp. 174-179.

[3] N. Ahmed, A. Haider, D. Van Hertem, Z. Lidong, and H. P. Nee, "Prospects and challenges of future HVDC SuperGrids with modular multilevel converters," in *Power Electronics and Applications (EPE 2011), Proceedings of the 2011-14th European Conference on*, 2011, pp. 1-10.

[4] B. Jacobsen, Karlsson, P., Asplund, G., Harnefors,L., Jonsson,T.,, "VSC-HVDC Transmission with cascaded Two-level Converters," in *CIGRE*, 2010.

[5] D. R. Trainer, Davidson, C. C., Oates, C. D. M., Macleod, N. M., & Critchley, D. R. , "A New Hybrid Voltage-Sourced Converter for HVDC Power Transmission," in *Cigre* 2010.

[6] M. M. C. Merlin, T. C. Green, P. D. Mitcheson, D. R. Trainer, R. Critchley, W. Crookes, *et al.*, "The Alternate Arm Converter: A New Hybrid Multilevel Converter With DC-Fault Blocking Capability," *Power Delivery, IEEE Transactions on*, vol. 29, pp. 310-317, 2014.

[7] R. Feldman, M. Tomasini, E. Amankwah, J. C. Clare, P. W. Wheeler, D. R. Trainer, *et al.*, "A Hybrid Modular Multilevel Voltage Source Converter for HVDC Power Transmission," *Industry Applications, IEEE Transactions on*, vol. 49, pp. 1577-1588, 2013.

[8] G. P. Adam, Finney, S. J., Williams, B. W.,Trainer, D. R.,Oates, C. D. M.,Critchley, D. R., "Network fault tolerant voltage-source-converters for high-voltage applications," in *AC and DC Power Transmission, 2010. ACDC. 9th IET International Conference on*, 2010, pp. 1-5.

[9] A. Lesnicar and R. Marquardt, "An innovative modular multilevel converter topology suitable for a wide power range," in *Power Tech Conference Proceedings, 2003 IEEE Bologna*, 2003, p. 6 pp. Vol.3.

[10] L. B. Feng Wang, Tuan Le, "An Overview of VSC-HVDC : State - of - art and potential applications in Electric Power Systems," *Cigre*, 2011.

[11] J D Ainsworth, M Davies, P J Fitz, K E Owen, and D. R. Trainer, "A static var compensator (STATCOM) based on single phase chain circuit convertors," *IEE Proceedings, Generation, Transmission and Distribution*, vol. 145, July 1998.

[12] C. C. Davidson and D. R. Trainer, "Innovative concepts for hybrid multi-level converters for HVDC power transmission," in *AC and DC Power Transmission, 2010. ACDC. 9th IET International Conference on*, 2010, pp. 1-5.

[13] A. Nabae, I. Takahashi, and H. Akagi, "A New Neutral-Point-Clamped PWM Inverter," *Industry Applications, IEEE Transactions on*, vol. IA-17, pp. 518-523, 1981.

[14] T. A. Meynard and H. Foch, "Multi-level conversion: high voltage choppers and voltage-source inverters," in *Power Electronics Specialists Conference, 1992. PESC '92 Record., 23rd Annual IEEE*, 1992, pp. 397-403 vol.1.

[15] J. J. M. B. D. Railing, P. Steckley, G. Moreau, P. Bard, L. Ronstrom, and J. Lindberg, "Cross Sound Cable Project : Second Gemeration VSC Technology for HVDC0," presented at the Cigre, 21, rue d'Artois, F-75008, Paris, 2004.

[16] X. Lie and V. G. Agelidis, "VSC Transmission System Using Flying Capacitor Multilevel Converters and Hybrid PWM Control," *Power Delivery, IEEE Transactions on*, vol. 22, pp. 693-702, 2007.

[17] B. R. Andersen, L. Xu, and K. T. G. Wong, "Topologies for VSC transmission," in *AC-DC Power Transmission, 2001. Seventh International Conference on (Conf. Publ. No. 485)*, 2001, pp. 298-304.

[18] A. Lesnicar and R. Marquardt, "A new modular voltage source Inverter topology," in *EPE2003*, 2003.

[19] E. K. Amankwah, J. C. Clare, P. W. Wheeler, and A. J. Watson, "Multi carrier PWM of the modular multilevel VSC for medium voltage applications," in *Applied Power Electronics Conference and Exposition (APEC), 2012 Twenty-Seventh Annual IEEE*, 2012, pp. 2398-2406.

[20] M. M. C. Merlin and T. C. Green, "Cell capacitor sizing in multilevel converters: cases of the modular multilevel converter and alternate arm converter," *Power Electronics, IET*, vol. 8, pp. 350-360, 2015.

[21] L. Xiaoqian, L. Wenhua, S. Qiang, R. Hong, and X. Shukai, "An enhanced MMC topology with DC fault ride-through capability," in *Industrial Electronics Society, IECON 2013 - 39th Annual Conference of the IEEE*, 2013, pp. 6182-6188.

[22] I. E. Commission, "High Voltage Direct Current (HVDC) Transmission using voltage source converters (VSC) " 2011.

[23] R. Feldman, E. Farr, A. J. Watson, J. C. Clare, P. W. Wheeler, D. R. Trainer, *et al.*, "DC fault ride-through capability and STATCOM operation of a HVDC hybrid voltage source converter," *Generation, Transmission & Distribution, IET*, vol. 8, pp. 114-120, 2014.

[24] A. M. Cross, D. R. Trainer, and R. W. Crookes, "Chain-link based HVDC Voltage Source Converter using current injection," in *AC and DC Power Transmission, 2010. ACDC. 9th IET International Conference on*, 2010, pp. 1-5.

[25] L. Haiwen, L. M. Tolbert, S. Khomfoi, B. Ozpineci, and D. Zhong, "Hybrid cascaded multilevel inverter with PWM control method," in *Power Electronics Specialists Conference, 2008. PESC 2008. IEEE*, 2008, pp. 162-166.

[26] E. K. Amankwah, J. C. Clare, P. W. Wheeler, and A. J. Watson, "Cell capacitor voltage control in a parallel hybrid modular multilevel voltage source converter for HVDC applications," in *Power Electronics, Machines and Drives (PEMD 2012), 6th IET International Conference on*, 2012, pp. 1-6.

[27] E. Amankwah, A. Watson, R. Feldman, J. Clare, and P. Wheeler, "Experimental validation of a parallel hybrid modular multilevel voltage source converter for HVDC transmission," in *Applied*

Power Electronics Conference and Exposition (APEC), 2013 Twenty-Eighth Annual IEEE, 2013, pp. 1607-1614.

[28] R. Feldman, M. Tomasini, J. C. Clare, P. Wheeler, D. R. Trainer, and R. S. Whitehouse, "A low loss modular multilevel voltage source converter for HVDC power transmission and reactive power compensation," in *AC and DC Power Transmission, 2010. ACDC. 9th IET International Conference on*, 2010, pp. 1-5.

[29] R. Feldman, Tomasini, M., Clare, J C., Wheeler, P. ,Trainer, D R. ,Whitehouse, R S.,, "A hybrid voltage source converter arrangement for HVDC power transmission and reactive power compensation," presented at the Power Electronics, Machines and Drives (PEMD 2010), 5th IET International Conference on, 2010.

[30] M. Tomasini, R. Feldman, J. C. Clare, P. Wheeler, D. R. Trainer, and R. S. Whitehouse, "DC-Link voltage ripple minimization in a modular multilevel voltage source converter for HVDC power transmission," in *Power Electronics and Applications (EPE 2011), Proceedings of the 2011-14th European Conference on*, 2011, pp. 1-10.

[31] J. Yang, Z. He, G. Tang, and H. Pang, "DC Voltage Compensation Strategy for Parallel Hybrid Multilevel Voltage Source Converter," *Power Delivery, IEEE Transactions on*, vol. PP, pp. 1-1, 2015.

[32] C. L. Fortescue, "Polyphase Power Representation by Means of Symmetrical Coordinates," *American Institute of Electrical Engineers, Transactions of the*, vol. XXXIX, pp. 1481-1484, 1920.

[33] C. L. Fortescue, "Method of symmetrical co-ordinates applied to the solution of polyphase networks," *American Institute of Electrical Engineers, Proceedings of the*, vol. 37, pp. 629-716, 1918.

[34] P. Rodriguez, J. Pou, J. Bergas, J. I. Candela, R. P. Burgos, and D. Boroyevich, "Decoupled Double Synchronous Reference Frame PLL for Power Converters Control," *Power Electronics, IEEE Transactions on*, vol. 22, pp. 584-592, 2007.

[35] R. H. Park, "Two-reaction theory of synchronous machines generalized method of analysis-part I," *American Institute of Electrical Engineers, Transactions of the*, vol. 48, pp. 716-727, 1929.

[36] R. K. Marian P. Kazmierskowski, frede Blaabjerg, *Control in Power Electronics; selected Problems*: Academic press, 2008.